Immunity, Volume *46*

Supplemental Information

Lymphocyte Circadian Clocks Control Lymph Node Trafficking and Adaptive Immune Responses

David Druzd, Olga Matveeva, Louise Ince, Ute Harrison, Wenyan He, Christoph Schmal, Hanspeter Herzel, Anthony H. Tsang, Naoto Kawakami, Alexei Leliavski, Olaf Uhl, Ling Yao, Leif Erik Sander, Chien-Sin Chen, Kerstin Kraus, Alba de Juan, Sophia Martina Hergenhan, Marc Ehlers, Berthold Koletzko, Rainer Haas, Werner Solbach, Henrik Oster, and Christoph Scheiermann

SUPPLEMENTAL INFORMATION

Figure S1

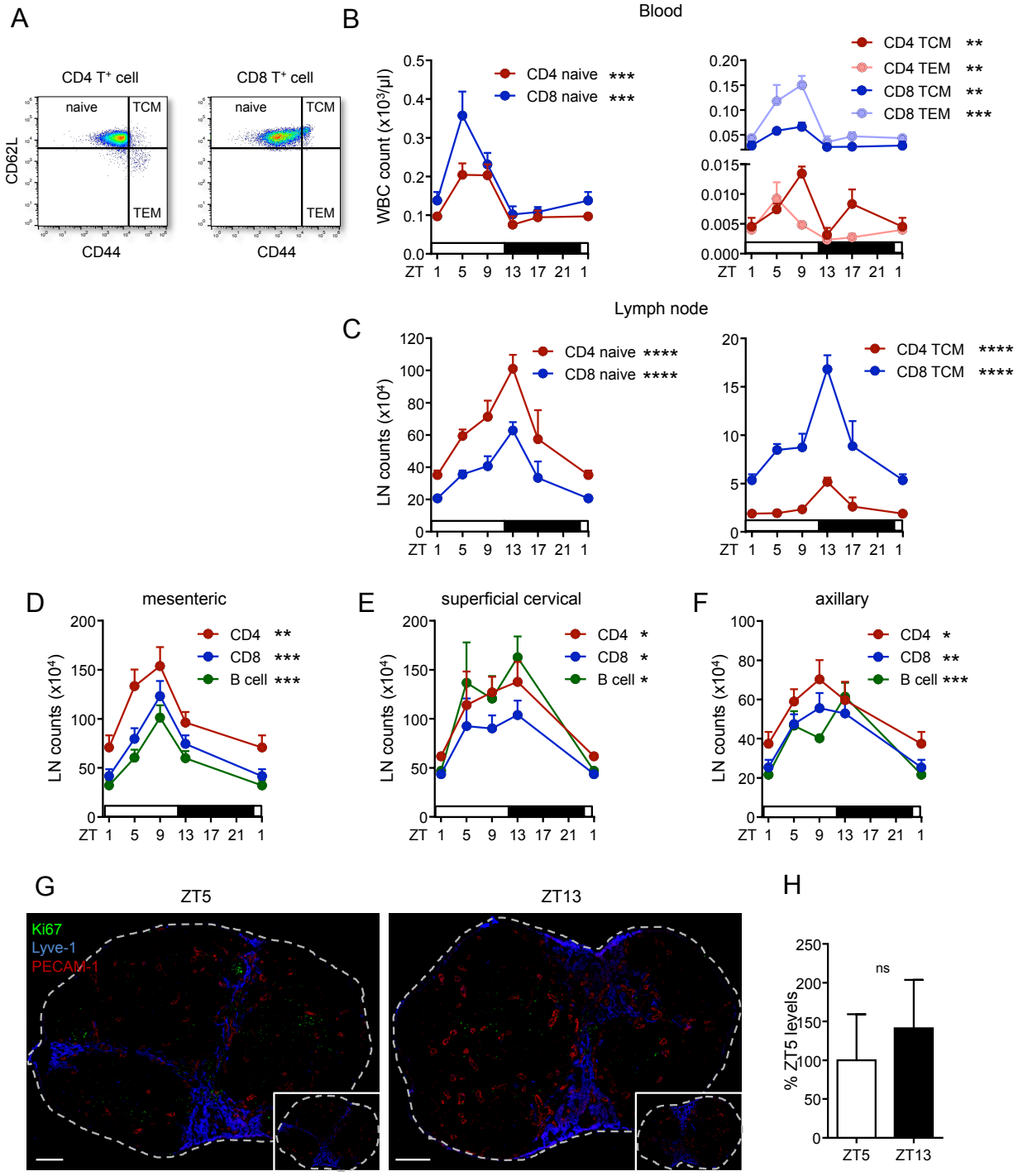

Figure S1, related to Figure 1

Oscillatory T lymphocyte subpopulations in blood and lymph node

(A-C) Gating strategy (gated on live cells) **(A)** and counts of naïve, central memory (TCM) and effector memory (TEM) CD4 and CD8 T lymphocytes in **(B)** blood (n=3-5 mice) and **(C)** lymph node (n= 6-18 mice); one-way ANOVA. **(D-F)** Counts of CD4 and CD8 T cells and B cells in **(D)** mesenteric lymph node (n=7-11 mice) **(E)** superficial cervical lymph node (n=4-7 mice) and **(F)** axillary lymph node (n=7 mice); one-way ANOVA. **(G)** Images of lymph node sections harvested at ZT5 and ZT13 and stained with antibodies directed against Ki67, PECAM-1, and Lyve-1. Inset: isotype antibody-stained control sections. Scale bars: 200 μm. **(H)** Quantification of $Ki67^+$ cells per lymph node section; n=4-5 mice. *p<0.05, **p<0.01, ***p<0.001, ****p<0.0001.

Figure S2

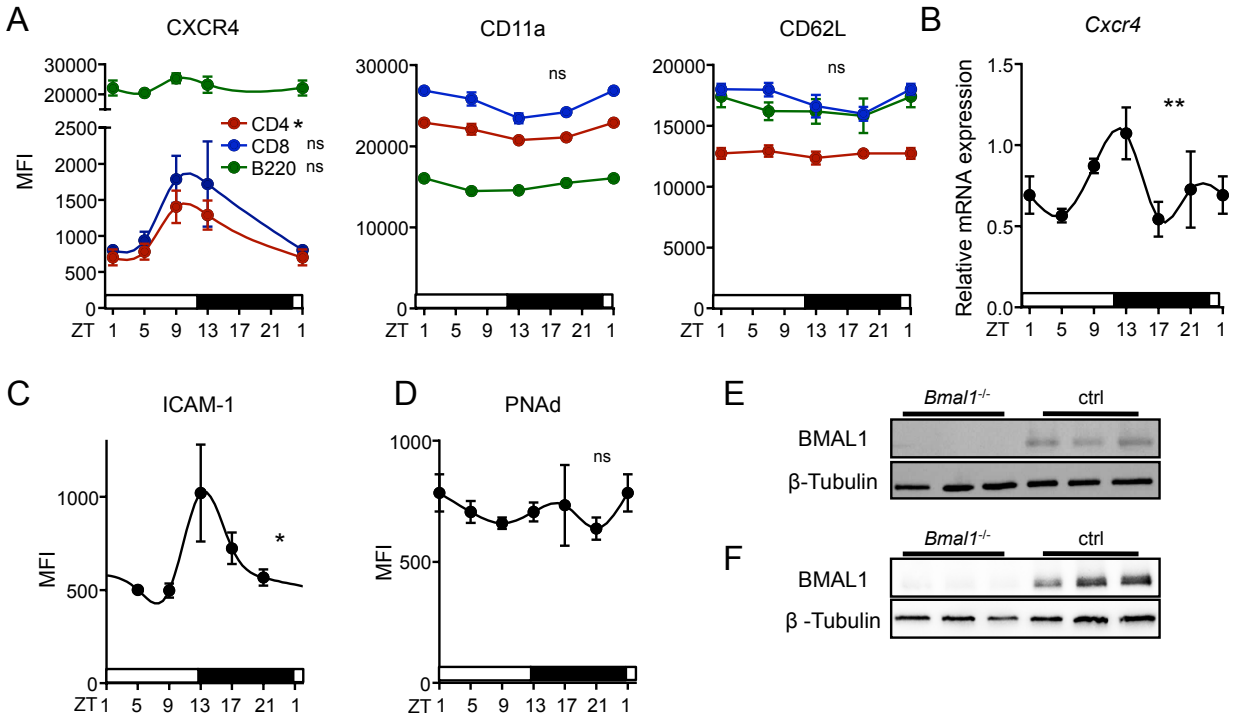

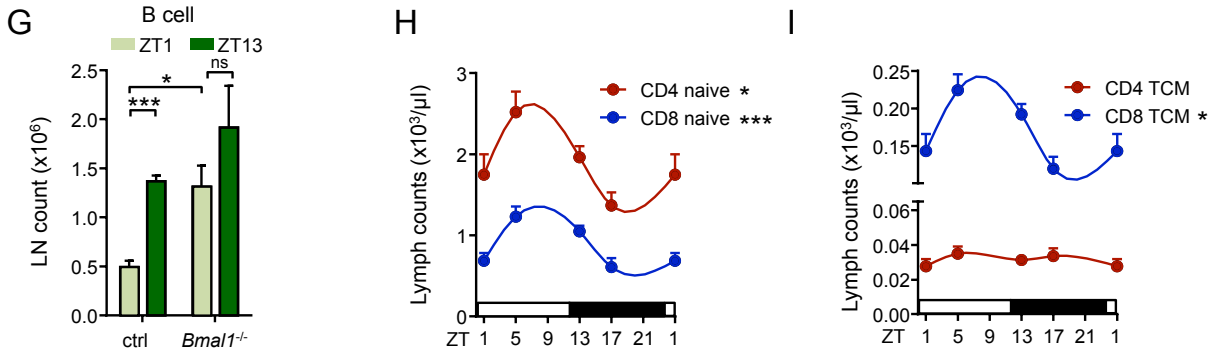

J

Time	ZT1	ZT7	ZT13	ZT21
Lymph volume (µl)	72 ± 5	70 ± 5	68 ± 4	79 ± 4
Lymph flow (µl/min)	1.2 ± 0.1	1.2 ± 0.1	1.1 ± 0.1	1.3 ± 0.1

Figure S2, related to Figures 2, 3 and 4

Oscillations of leukocyte promigratory factors and numbers

(A) Oscillations in protein surface expression on lymphocyte subpopulations in lymph nodes; CXCR4, CD11a, CD62L; n=3-5 mice, one-way ANOVA; MFI, mean fluorescence intensity. **(B)** Q-PCR analysis of LN *Cxcr4* over 24h; n=3-5 mice, one-way ANOVA. **(C-D)** Quantification of expression of ICAM-1 **(C)** and PNAd **(D)** on HEV over 24h in constant darkness (CT, circadian time: the corresponding light and dark phase are indicated); n=3 mice, one-way ANOVA. **(E)** Amount of BMAL1 protein in isolated splenic T cells from T cell specific *Bmal1*$^{-/-}$ and control animals; n = 3 mice, each lane represents an individual animal. **(F)** Amount of BMAL1 protein in isolated splenic B cells from B cell specific *Bmal1*$^{-/-}$ and control animals, each lane represents a technical replicate. **(G)** Lymph node B cell counts in control and B-cell-specific *Bmal1*$^{-/-}$ mice; n=3-4 mice, unpaired student's t-test. **(H-I)** Counts of naïve and central memory (TCM) CD4 and CD8 T lymphocytes in lymph; n=5-17 mice, one-way ANOVA. **(J)** Harvested lymph volume and flow rate over 24h; n=7-22 mice. *p<0.05, **p<0.01, ***p<0.001.

Figure S3

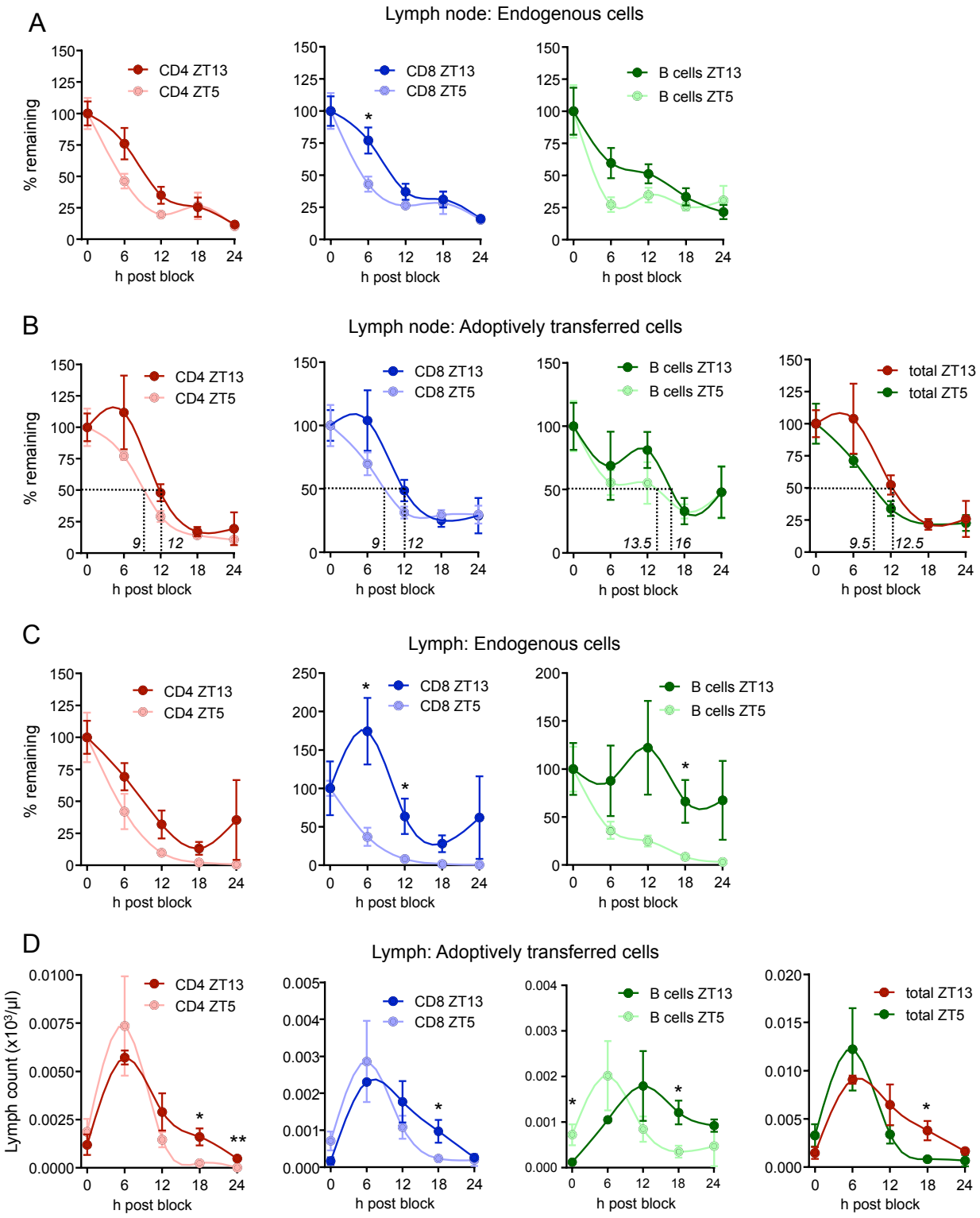
A
Lymph node: Endogenous cells
CD4 ZT13
CD4 ZT5
CD8 ZT13
CD8 ZT5
B cells ZT13
B cells ZT5
% remaining
h post block
B
Lymph node: Adoptively transferred cells
total ZT13
total ZT5
9
12
13.5
16
9.5
12.5
C
Lymph: Endogenous cells
D
Lymph: Adoptively transferred cells
Lymph count (x10³/µl)

Figure S3, related to Figure 4

Analysis of oscillations in lymph node half life

Change in cellular numbers (in % **(A-C)**) or absolute numbers **(D)** of endogenous **(A** and **C)** and adoptively transferred **(B** and **D)** leukocytes in lymph node and lymph over 24h after block of leukocyte homing. Lymph node: n= 3-10 mice; lymph: n=3-6 mice, unpaired student's t-test. *$p<0.05$, **$p<0.01$.

Figure S4

For the sake of simplicity, it was assumed that both homing and egress rhythms follow a sinusoidal oscillation with a certain amplitude and phase. The individual phases were termed Φ_h and Φ_e, respectively.
Let $x(t)$ be the time-dependent lymphocyte count in the lymph node:

$$dx(t)/dt = g(t) - l(t) \quad (1)$$

Here, the time-dependent gain rate is represented by $g(t)$ and can be summarised as a non-negative sinusoidal function of the form:

$$g(t) = A(1 + \sin(\omega t + \Phi_h)) \quad (2)$$

where A is amplitude and ω is angular frequency. The time-dependent loss rate is represented by $l(t)$ and can be replaced by a non-negative sinusoidal function of the form:

$$l(t) = d(1 + \sin(\omega t + \Phi_e))\, x(t) \quad (3)$$

where d is decay rate and other nomenclature remains the same.

Using these formulae, a model for circadian homing with the egress replaced with a simple exponential decay rate can be summarised as:

$$dx(t)/dt = A(1 + \sin(\omega t + \Phi_h)) - dx(t) \quad (4)$$

A model for circadian egress with a fixed gain rate can be summarised as:

$$dx(t)/dt = A - d(1 + \sin(\omega t + \Phi_e))\, x(t) \quad (5)$$

A model where both homing and egress oscillate can be summarised as:

$$dx(t)/dt = A(1 + \sin(\omega t + \Phi_h)) - d(1 + \sin(\omega t + \Phi_e))\, x(t) \quad (6)$$

Model parameters were estimated by fitting to time series data obtained under steady state and blocked homing conditions. Time series data obtained under a blocked egression was spared from the fitting and taken as a cross-validation. Comparisons of modelled and actual data in steady state conditions are shown in Figure 4G (total cell count) and below (individual subsets).

The relative quality of the models given our set of data was tested by means of the Akaike information criterion (AIC), using the formula commonly used for regression models. Its value can be given by:

$$AIC = N \ln(X^2/N) + 2K \quad (7)$$

where N is the number of data points, K is the number of parameters plus one, and X^2 is the residual sum of squares. Models with smaller numbers of AIC values are assumed to outperform those with higher values.

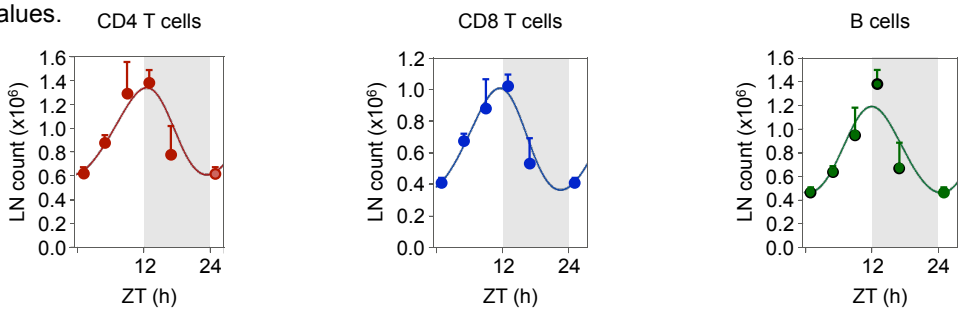

Figure S4, related to Figure 4

Mathematical modeling of cellular oscillations in lymph nodes

Formulas and fits for optimal modeling parameter sets (curves) vs. actual data sets (points) for steady-state oscillations of CD4 and CD8 T cells and B cells using the dual oscillation mathematical model that incorporates rhythmic homing to LNs and rhythmic egress from LNs. The ZT1 time point has been double-plotted to facilitate viewing.

Figure S5

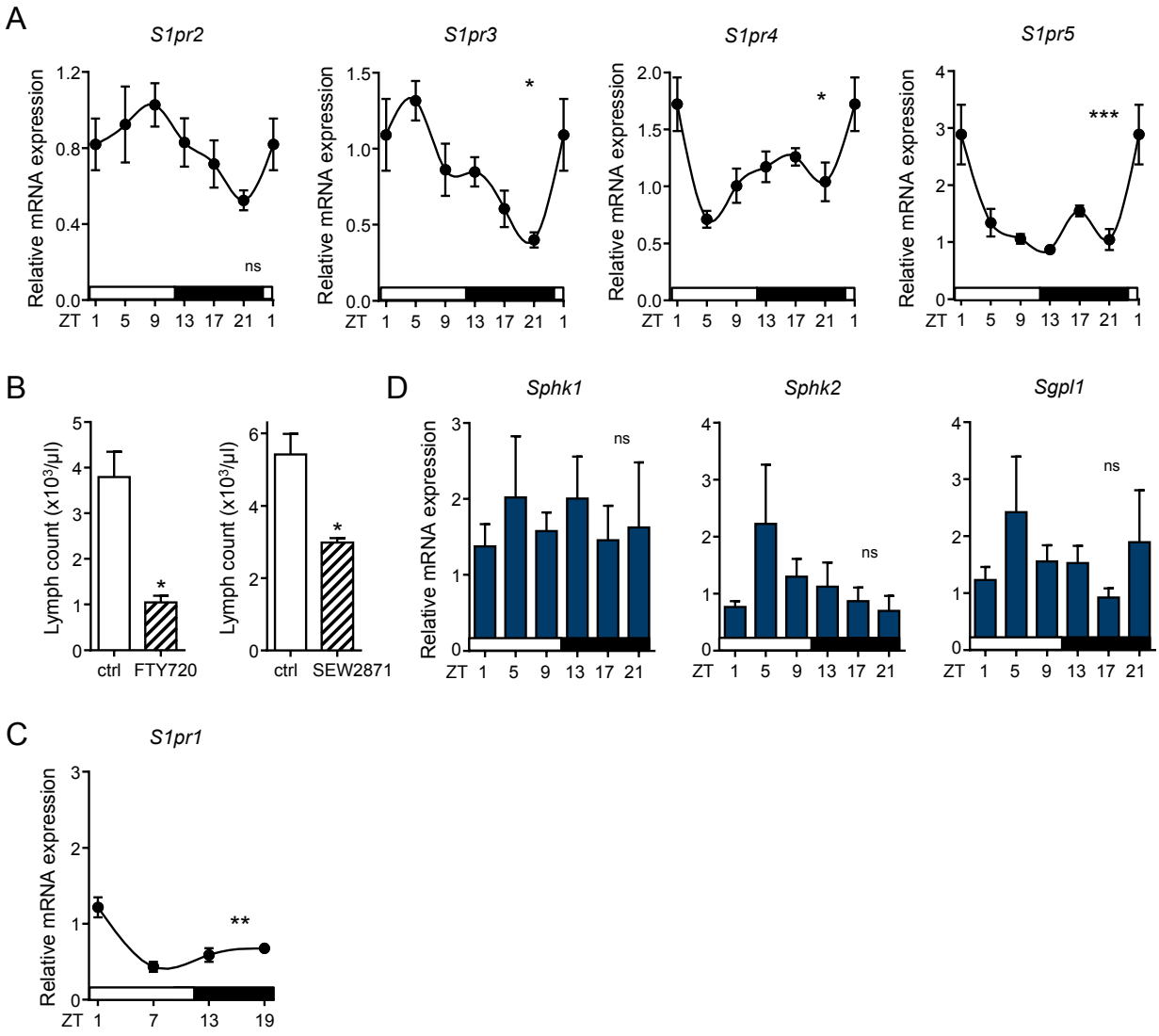
A
S1pr2
S1pr3
S1pr4
S1pr5
Relative mRNA expression
ns
*
*
***
ZT 1 5 9 13 17 21 1
B
Lymph count (x10³/µl)
ctrl FTY720
ctrl SEW2871
D
Sphk1
Sphk2
Sgpl1
ns
ns
ns
ZT 1 5 9 13 17 21
C
S1pr1
**
ZT 1 7 13 19

Figure S5, related to Figure 5

Diurnal expression profiles of *S1pr* genes

(A) Q-PCR analysis of LN *S1pr2*, *S1pr3*, *S1pr4* and *S1pr5* over 24h; n=3-5 mice, one-way ANOVA. **(B)** Lymph counts in control animals or animals treated with FTY720 or SEW2871; n=3-6 mice, unpaired student's t-test. **(C)** Q-PCR analysis of *S1pr1* in CD4 T cells isolated from *S1pr1*$^{+/-}$*xCd4-cre* mice over 24h; n=3 mice, one-way ANOVA. **(D)** Q-PCR analysis of LN Sphingosine kinase 1 and 2 (*Sphk1* and *Sphk2*) and Sphingosine-1-phosphate lyase *(Sgpl1)* over 24h; n=3-5 mice, one-way ANOVA. *p<0.05, **p<0.01, ***p<0.001.

Figure S6

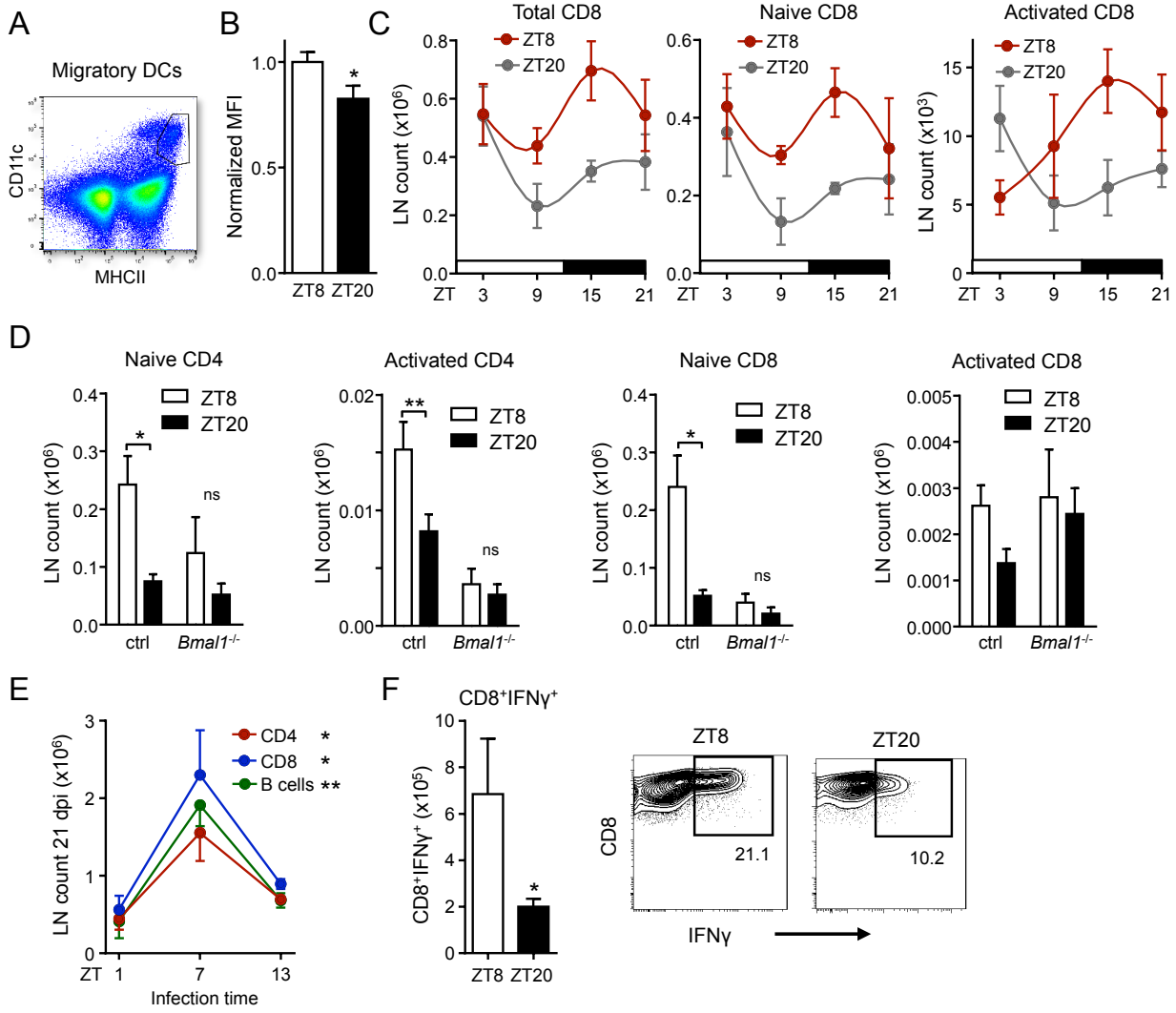
A
Migratory DCs
CD11c
MHCII
B
Normalized MFI
ZT8 ZT20
C
Total CD8
Naive CD8
Activated CD8
ZT8
ZT20
LN count (x10^6)
LN count (x10^3)
ZT 3 9 15 21
D
Naive CD4
Activated CD4
Naive CD8
Activated CD8
LN count (x10^6)
ctrl
Bmal1-/-
ns
E
CD4 *
CD8 *
B cells **
LN count 21 dpi (x10^6)
Infection time
F
CD8+IFNγ+
CD8+IFNγ+ (x10^5)
ZT8
ZT20
CD8
IFNγ
21.1
10.2

Figure S6, related to Figure 6

Diurnal rhythmicity in experimental autoimmune encephalomyelitis (EAE)

(A) Gating strategy (gated on live singlet cells) of migratory DCs. (**B**) Proliferation of MOG-specific T cells as analyzed by *in vivo* immunization of mice at ZT8 and ZT20, followed by dye-dilution analyses after re-stimulation with the antigen in culture; n=10 mice, unpaired student's t-test. **(C)** Diurnal profiles of inguinal lymph node counts of total CD8 T cells, naïve CD8 T cells, and activated CD8 T cells on day 2 after EAE induction; n=4 mice. Black and white bars indicate the dark and light periods, respectively **(D)** Naïve and activated CD4 and CD8 T cell counts in inguinal lymph nodes sampled at ZT15 on the second day after EAE induction; n=4-5 mice, unpaired student's t-test. **(E)** Lymph node counts of mice that were infected at different times of the day (ZT1, ZT7 or ZT13) with *Helicobacter pylori* and harvested at one time 21 days post infection (dpi); n=4 mice, one-way ANOVA. **(F)** Pulmonary $CD8^{+}IFN\gamma^{+}$ T cells of mice infected with influenza A virus at different times of the day (ZT8 and ZT20). Lungs were harvested 8 dpi and infiltrating T cells were enumerated and IFNγ production was assessed by flow cytometry; n=4 mice, Mann-Whitney test. *$p<0.05$, **$p<0.01$.

Primers	Sequence	Annealing(°C)
Bmal1_F	AGA GGT GCC ACC AAC CCA TA	62
Bmal1_R	TGA GAA TTA GGT GTT TCA GTT CGT CAT	
Bmal1_F	CCT AAT TCT CAG GGC AGC AGA T	60
Bmal1_R	TCC AGT CTT GGC ATC AAT GAG T	
Clock_F	CAA AAT GTC ACG AGC ACT TAA TGC	62
Clock _R	ATA TCC ACT GCT GGC CTT TGG	
Per1_F	TGA GAG CAG CAA GAG TAC AAA CTC A	60
Per1_R	CTC GCA CTC AGG AGG CTG TAG	
Per2_F	GTC CAC CTC CCT GCA GAC AA	60
Per2_R	TCA TTA GCC TTC ACC TGC TTC AC	
Cry1_F	CTC GGG TGA GGA GGT TTT CTT	62
Cry1_R	GAC TTC CTC TAC CGA GAG CTT CAA	
Nr1d1_F	GAT AGC TCC CCT TCT TCT GCA TCA TC	60
Nr1d1_R	TTC CAT GGC CAC TTG TAG ACT TC	
Nr1d1_F	AGC TCA ACT CCC TGG CAC TTA C	60
Nr1d1_R	CTT CTC GGA ATG CAT GTT GTT C	
Dbp_F	AAT GAC CTT TGA ACC TGA TCC CGC T	60
Dbp_R	GCT CCA GTA CTT CTC ATC CTT CTG T	
S1pr1_F	CGG TGT AGA CCC AGA GTC CT	64
S1pr1_R	AGC AGC AGA TGA GAA TGA AC	
S1pr2_F	ATG GGC GGC TTA TAC TCA GAG	60
S1pr2_R	GCG CAG CAC AAG ATG ATG AT	
S1pr3_F	TTC CCG ACT GCT CTA CCA TC	62
S1pr3_R	CCA ACA GGC AAT GAA CAC AC	
S1pr4_F	TGC GGG TGG CTG AGA GTG	62
S1pr4_R	TAG GAT CAG GGC GAA GAC C	
S1pr5_F	CTT AGG ACG CCT GGA AAC C	62
S1pr5_R	CCC GCA CCT GAC AGT AAA TC	
Ccr7_F	TCA TTG CCG TGG TGG TAG TCT TCA	62
Ccr7_R	ATG TTG AGC TGC TTG CTG GTT TCG	
Cxcr4_F	TCA GTG GCT GAC CTC CTC TT	60
Cxcr4_R	CTT GGC CTT TGA CTG TTG GT	
Ccl21_F	ACA GCG GCC TCC AGA AGA ACA GCG G	64
Ccl21_R	CGT GAA CCA CCC AGC TTG A	
Gapdh_F	TGT GTC CGT CGT GGA TCT GA	60
Gapdh_R	CCT GCT TCA CCA CCT TCT TGA	
Eef1a_F	TGC CCC AGG ACA CAG AGA CTT CA	60
Eef1a_R	AAT TCA CCA ACA CCA GCA GCA A	
Sphk1_F	GAAGACCTGCTCATCAACTGC	60
Sphk1_R	GTGCCCACTGTGAAACGAA	
Sphk2_F	TAGATGGGGAGTTAGTGGAGTATG	60
Sphk2_F	TGCTTTTAGGCTCGTTCAGG	
Sgpl1_F	TGATGGCCTGCAAAGCTT	60
Sgpl1_R	GCCACAATTTCTGGAGTTTTGA	
Il2_F	AACCTGAAACTCCCCAGGAT	60
Il2_R	CGCAGAGGTCCAAGTTCATC	

Q-PCR primer sequences, related to Figure 2, 3, 5, 6, S2, S5

Movie S1

Movie showing the circadian migration of lymphocytes through lymph nodes. At night onset, increased homing due to higher amounts of lymphocyte CCR7 leads to enhanced lymphocyte counts in the lymph node. During the day, higher *S1pr1* expression induces the egression of lymphocytes into efferent lymph.

SUPPLEMENTAL EXPERIMENTAL PROCEDURES

Antibodies

Antibodies targeting the following antigens were used: CD3e (clone 145-2C11; Biolegend), CD3 (17A2; Biolegend), CD4 (GK1.5; Biolegend), CD8a (53-6.7; Biolegend), CD16/32 (2.4G2; BD Biosciences), CD44 (IM7; Biolegend), CD45 (30-F11; Biolegend), CD62L (MEL-14; Biolegend), B220 (RA3-6B2; Biolegend), NK1.1 (PK136; Biolegend), Gr-1 (RB6-8C5, Biolegend), CD11b (M1/70; Biolegend), CD11c (N418; Biolegend), MHCII I-A/I-E (M5/114.15.2, Biolegend); CCR7 (4B12; Biolegend), CXCR4 (L276F12; Biolegend), CD11a (M17/4; Biolegend), IL-17A (TC11-18H10, BD Horizon), CD49d (R1-2, Biolegend), Ki67 (SolA15; eBioscience), PECAM-1 (Mec13.3; Biolegend), Lyve-1 (ALY7; eBioscience), CCL21 (goat anti-mouse polyclonal; R&D Systems), ICAM-1 (YN1/1.7.4; Biolegend), PNAd (MECA-79, Biolegend), blocking antibodies against CD49d (PS/2) and CD11a (M17/4; both BioXCell), BMAL1 (NB 100-2288; Novus Biologicals), beta-tubulin (ab6046; Abcam).

Mass spectrometry analyses

Proteins of 20 µL sample matrix were precipitated by adding 200 µL methanol including D-erythro-sphingosine-1-phosphate C17 base (860641P, Avanti Polar Lipids) as internal standard. After centrifugation the supernatant was used for the analysis of S1P by liquid chromatography mass spectrometry (LC-MS/MS) analyses with a 1200 SL HPLC system (Agilent) coupled to a 4000QTRAP tandem mass spectrometer (AB Sciex). Separation was achieved with a Zorbax SB-C18, particle size 3.5 µm, 150 mm × 2.1 mm HPLC column (Agilent) and water with 0.1% formic acid as mobile phase A and methanol/ isopropanol (1:1) with 0.1% formic acid as mobile phase B. A gradient elution was used for optimal separation from 60% B to 80% B within 7 minutes. After column cleaning at 100% B for 1 minute, the gradient was equilibrated for 2.5 min at 60% B before the next injection. The LC-MS/MS system operated in positive electrospray ionization with electron voltage of 5500V at 400 °C. Auxiliary gas was set to 50 psi and 60 psi was used for nebulizer gas. Curtain gas was set to 30 psi and collision gas was set to 8 psi. Mass transitions and individual energies (declustering potential, collision energy, collision cell exit potential) were optimized by direct infusion and set as follows: m/z 380.2→264.2 (66, 23, 18) and 380.2→82.1 (66, 49, 6) for S1P and 366.2→250.2 (61, 23, 18) and 366.2→82.0 (61, 45, 6) for internal standard. Mass transitions were detected in multiple reaction monitoring mode with a dwell time of 100 ms. Quantification was achieved by standard calibrating curves prepared from D-erythro-sphingosine-1-phosphate C18:1 base (860492P, Avanti Polar Lipids) at different concentration points in the range from 0.005 to 0.5 µmol/L.

Western blotting

To obtain total cell lysates, MACS-purified T cells were incubated with RIPA buffer (150 mM NaCl; 50 mM Tris-HCl, 0.1 % SDS, 0.5 % Na-Dox, 0.1 % SDS, 1 % NP40, 1 mM EDTA, and proteinase inhibitor). Nuclei were pelleted in a microfuge at 14,000 x g for 15 min, and the supernatant was used as the cytoplasm fraction. Cell lysates were normalized by measuring total protein concentrations using the Pierce BCA Protein Assay Kit (Thermo Scientific) according to the manufacturer's protocol. Proteins were separated on a 10 % SDS-PAGE and transferred to PVDF membranes (Roche). Membranes were blocked in 5 % milk powder for 1 h and then probed with anti-BMAL1 antibody (1:2000 in 5 % milk-TBS; NB 100-2288, Novus Biologicals, Littleton, USA) overnight at 4 °C. Anti-β-Tubulin antibody (Abcam) was used for normalisation. HRP-conjugated anti-rabbit or anti-mouse IgGs were used as secondary antibodies. Proteins were visualized by enhanced chemiluminescence (Thermo, No. 34080) and a Fusion SL Image Acquisition System (Vilber Lourmat).

Histology

Mice were perfused intracardially with ice-cold PBS followed by fixation with 4% paraformaldehyde (PFA) for 10 minutes. Spinal cords were post-fixed overnight and then dissected from the spinal canal. Paraffin embedded 10-µm transverse sections of the lumbar spinal cord were stained for total myelin with Luxol Fast Blue Stain/ Cresyl Echt Violet (Abcam) according to the manufacturer's instructions, dehydrated, cleared with xylene, and mounted for microscopy. Images of lumbar spinal cord were taken at levels L1/2, L3/4 and L5/6 for each mouse and demyelinated areas measured using ImageJ software (National Institutes of Health).

Quantitative real-time PCR

RNA was extracted using RNeasy Plus Mini Kit (Qiagen) or with TRIzol reagent (Life Technologies), in accordance with the manufacturers' instructions. Reverse transcription was carried out using the High Capacity cDNA Reverse Transcription Kit (Applied Biosystems), in accordance with the manufacturer's instructions. Q-PCR was performed with SYBR GREEN on a StepOnePlus Real-Time PCR System (Applied Biosystems). A primer concentration of 0.5µM was found to be optimal in all cases. The sequences of the oligonucleotides used are included in the Supplemental Experimental Procedures. The PCR protocol consisted of one cycle at 95 °C (10 min) followed by 40 cycles of 95 °C (15 s) and 60-64 °C (1 min). Expression of glyceraldehyde-3-phosphate dehydrogenase (GAPDH) was generally used as a standard. For EAE experiments Q-PCR was conducted with the GoTaq Q-PCR Master Mix (Promega) and a CFX96 Real-Time PCR Detection System (Bio-Rad) according to the manufacturer's instructions, along with gene-specific primers. Eef1a was used as reference gene. Relative quantification was performed using the ΔΔCT method.

T-cell proliferation analyses

Spleens were harvested from mice 10 days after EAE immunization. CD3+ T cells were negatively selected using the Pan T Cell Isolation Kit II (Miltenyi Biotec) and labelled with a proliferation dye (CellTrace™ Violet Cell Proliferation Kit, Life Technologies). T-cell depleted splenocytes (1×10^5/well) isolated from EAE mice were

cultured in the presence or absence of the MOG peptide (10 µg/ml) or irrelevant peptide (ovalbumin) (10 µg/ml) or no antigen at 37℃ in 5% CO2 for 1 h. CD3+ T cells were co-cultured with antigen-pulsed splenocytes at 37°C in 5% CO2 for 3 days RPMI medium 1640 supplemented with 10% FCS, 10mM HEPES and 55µM beta-mercaptoethanol in 96-well flat-bottom plates, at 2×10^5 cells per well.

Helicobacter pylori infection

Mice were infected orogastrically at ZT1, ZT7 and ZT13 with the H. pylori strain PMSS1wt with a dose of 109 bacteria. Animals were sacrificed after 3 weeks and LN cellularity was analyzed by flow cytometry.

Influenza A virus infection

Female 8-10 week old C57B/6 (CD45.1+) mice were intranasally infected with 100 plaque forming units (pfu) of Influenza A virus (strain A/Puerto Rico/8/1934 H1N1) at ZT8 and ZT20. Animals were sacrificed on day 8 post infection and lymphocyte infiltration and activation was assessed in lung tissue homogenates by flow cytometry. Animal experiments were approved by the local animal ethics committee (LAGeSo).